Military Technical College
Kobry El-Kobbah,
Cairo, Egypt.

16th International Conference on Applied Mechanics and Mechanical Engineering.

MODELING AND SIMULATION OF HYBRID ELECTRIC VEHICLES

A. M. Ali *, H. M. Kamel*, A. M. Sharaf *, and S. A. Hegazy*

ABSTRACT

This paper presents a detailed Hybrid Electric Vehicle (HEV) modelling method based on a multi-physics approach. The model is introduced in order to provide design engineers with the capability to investigate effects of component selection and to develop control systems and automatic optimization processes for HEVs. A full drivetrain system of a series/parallel HEV is developed including the internal combustion engine (ICE), the motor generator (MG) and the power split device (PSD) along with the vehicle longitudinal dynamics. All aspects of rotational inertial dynamics, friction, damping and stiffness properties are considered. The interaction between all these modules is implemented in the MATLAB/Simulink/Simscape blockset environment. The concepts of modularity, flexibility, and user-friendly interface are emphasized during the model development. The numerical simulation results are compared with the analytical results of the same hybrid power train. The convergence between the results makes the model convenient for the future optimization techniques on HEV.

KEY WORDS

Hybrid vehicles, MATLAB/SIMULINK, modelling, simulation, PSD.

NOMENCLATURE

A	Frontal area of the vehicle
C_d	Air drag coefficient
F_{in}	Required tension force
F_{xf}, F_{xr}	Tractive effort of the vehicle at front and rear axle, respectively
I_b	Batteries current
I_w, J	Tire and motor mass moment of inertia
M_d	Driving moment
R_c, R_s, R_r	Carrier, sun and ring gear radii respectively

---

* Egyptian Armed Forces.

T	Motor or braking torque
V	Battery or applied voltage
V_b	Batteries voltage
V_D	Air velocity
V_o	Initial battery charge
V_x	Vehicle longitudinal speed
X	The ratio of the ampere-hours left to the rated ampere-hours
f	Rolling resistance coefficient
k_t, k_v	Torque and back emf constants
m	Vehicle mass
r_d	Dynamic radius of the vehicle
ξ_{RS}	Ring to sun gear ration of the PSD
α, β	empirical constants
β	Ground surface inclination
Ω	Tire rotational speed
$\omega_c, \omega_s, \omega_r$	Ring, sun and carrier gear speed (rpm) respectively
ω_{th}	Angular velocity threshold
ρ	Air density
γ	Motor damping
μ	contact friction coefficient
φ	wrap angle

INTRODUCTION

Over the past decade, the lack of petroleum resources and the increased emission rates have stimulated the automotive research all over the world to find more sustainable and clean energy resources. While the limited fossil fuel reserves are being continuously depleted, both the demand and the production rates are growing rapidly [1-2]. Hybrid Electric Vehicle (HEV) has been considered as a short term solution to not only improve the fuel economy but also reduce its harmful emissions [3]. It is wildly known that, HEV combines two sources of energy namely; the conventional ICE and the electric propulsion systems which in turn reduce the dependency on petroleum fuels. Furthermore, the concept of having dual power sources enables the engine downsizing, load leveling and range extending. Proper engine sizing enables running the engine near to its economic conditions, regardless of the vehicle's required power and accordingly less emission levels [4].

Generally, according to the architecture of hybrid propulsion, there are three basic layouts of HEVs namely; series, parallel and series/parallel HEVs. In series HEV, the mechanical energy is produced by the engine and converted to electric energy through the generator. This electric energy is stored in the battery pack and again is

converted to mechanical energy via the electric motors to propel the vehicle as illustrated in Figure 1-a. Ease of both installation and operation are the main features of this type but double energy conversion represents its major disadvantages. Also, the series power flow reduces the powertrain redundancy. In parallel HEV, both the mechanical power from the engine and electric power from the motor are combined to drive the vehicle as shown in Figure 1-b. While this layout provides more choices of operation, it is practically complex to implement in the drivetrain. Series/parallel HEV layout joins the advantages of the aforementioned layouts and provides the choice of utilizing both the mechanical and electric energies either sequentially or simultaneously. Nevertheless, the construction complexity is one of its main drawbacks as shown in Figure 1-c.

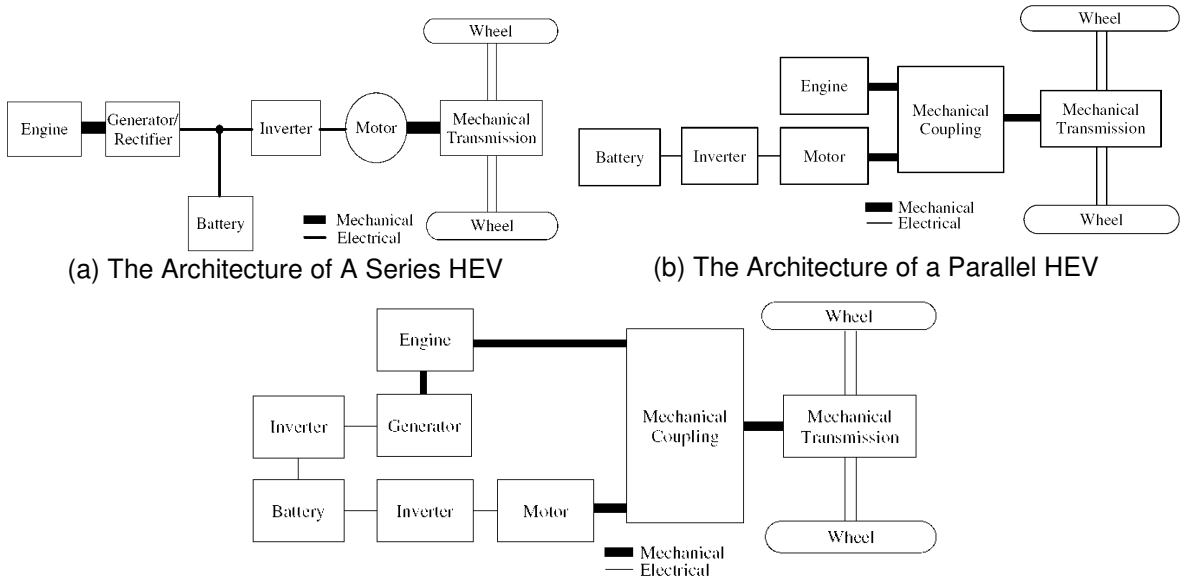

(a) The Architecture of A Series HEV

(b) The Architecture of a Parallel HEV

(c) The Architectures of a Series/Parallel HEV

Fig. 1 Hybrid Vehicle Topologies.

Accurate modeling and simulation of HEVs enables better understanding and control of their operation. Among the well-known published literature, Khan developed a model for '*Honda Integrated Motor Assist*' (IMA) in MATLAB/Simulink environment [5]. Three parameters were considered and compared during two different standard drive cycles; these are fuel consumption, regenerated energy and consumed energy. Peng and Liu introduced an optimization algorithm for the series/parallel '*Toyota Hybrid System*' (THS) [1,6]. Later, they discussed the argument between improvements of component sizing or powertrain architecture for '*Toyota Hybrid System*' (THSII) considering rule based optimization [7-9]. Peng et al. developed another control algorithm for the model of parallel HEV considering adaptive energy management control system [10]. Stein et al. introduced a MATLAB/ Simulink model to apply a dynamic programming algorithm [11]. Using ADVISOR, Wipke et al. developed a simulator to simulate the full HEV powertrain [12]. While, the reviewed work has contributed to the state of the art in HEV, it should be noted that, most of them were either dedicated to a certain hybrid topology [1, 5, 6] or constrained to limited access simulator [9]. However, there is a need to develop more generic models, yet adequate to represent HEV performance accurately. A simplified model is presented in this paper with a code such that it is accessible to modify its sub-

systems and subjected for further optimization techniques. Particular attention is paid to the modelling of series/parallel HEV due to its wide application in modern vehicles.

THE MODEL DISCRIPTION

The core of the series/parallel HEV is a power split device which combines the power from the engine and the electric motor generator (MG). The output power from PSD is then delivered to the wheels through transmission elements such as propeller shaft, open differential and back axle as shown in Figure 2.

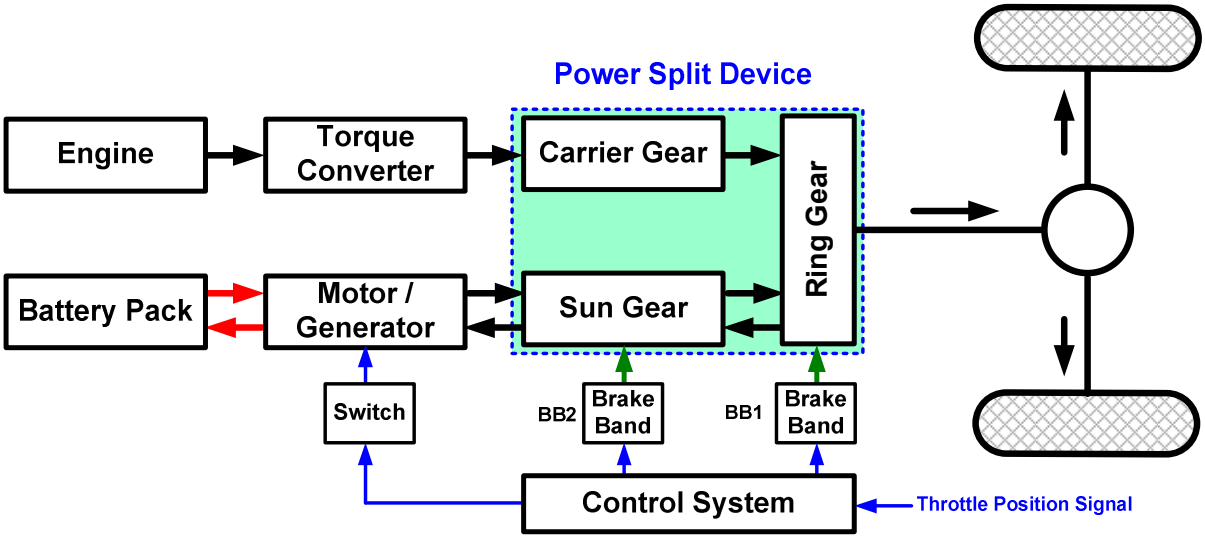

Fig. 2 The Main Layout of the HEV Model.

These elements are modeled and implemented using Simscape blockset library including SimDriveline, SimElectronics and SimPowerSystems toolboxes [17]. Simscape blockset is a part of Simulink physical modelling, encompassing the modelling and design of systems according to basic physical principles. Physical modelling runs within the Simulink environment and interfaces seamlessly with the rest of Simulink and with MATLAB. Unlike other Simulink blocks, which represent mathematical operations, physical modelling blocks represent physical components or relationships directly such that, it is possible to represent a HEV drivetrain system with a connected block diagram.

The engine characteristics are included in the model as a look-up table of engine torque versus engine speed and throttle position, see Figure 3. Rotational motion can be initiated and maintained in a driveline with actuators while measuring, via sensors, the motions of driveline elements and the torques acting on them. The torque converter is modelled with the physical characteristics shown in Figure 4.

The model of the DC motor's equivalent circuit is represented by the armature resistance (R). For the steady-state torque-speed relationship the inductance (L) is

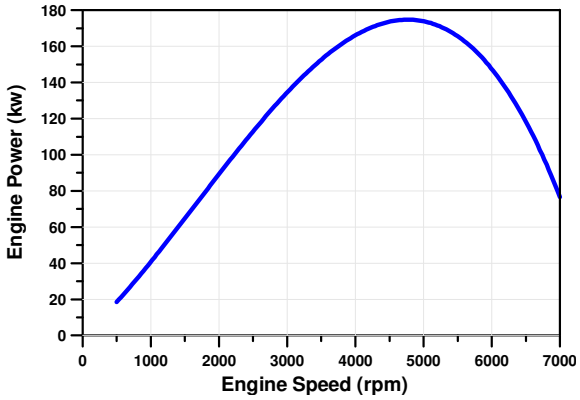

Fig. 3. Engine Characteristics.

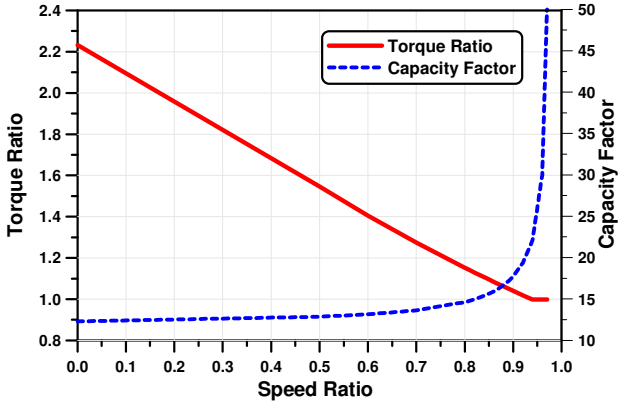

Fig. 4. Torque Converter Characteristics.

assumed to have no effect. Considering the motor inertia (J) and damping(γ), the resultant torque by the DC motor (T) is proportional to the armature current, the strength of the magnetic field and rotational speed (ω) as follows:

$$T = k_t \cdot \underbrace{\left(\frac{V - k_v \cdot \omega}{R}\right)}_{Armature\ Current} - J \cdot \dot{\omega} - \gamma \cdot \omega \tag{1}$$

where, (k_t, k_v) are the torque and back emf constants, $(k_v \cdot \omega)$ is the induced back voltage in the armature.

The battery model implements a generic dynamic model parameterized to represent most popular types of rechargeable batteries. The battery is modeled as a series resistor with a charge-dependent voltage source whose voltage is given as a function of charge of the following reciprocal relationship. For a given battery nominal voltage(V_o), the voltage across the battery terminals (V) is calculated as follows:

$$V = V_o \cdot \left(1 - \frac{\alpha \cdot (1-x)}{1 - \beta \cdot (1-x)}\right) \tag{2}$$

where (x) is the ratio of the ampere-hours left to the rated ampere-hours of the battery, (α, β) are empirical constants. The initial and maximum states of charge of the battery are mentioned in table1.

The power split device (PSD) is a key component that directly controls the power flow among the engine and electric motor. The model of PSD considers a single-row planetary gear mechanism consisting of three basic components; a sun gear which is connected to the MG, a planet carrier equipped with planetary gear which is connected to the ICE and a ring gear which resembles the output to rear axle. Depending on which shaft is driving, driven, or fixed, the planetary gear train can achieve a variety of speed reduction ratios. These ratios are a function of the sun and ring radii$(\xi_{RS} = R_R / R_S)$, and therefore of their tooth numbers. The planetary

gear imposes two kinematic and two geometric constraints on the three connected axes and the fifth constraint; the internal wheel (planet), as shown in figure 5 [18].

$$R_C \cdot \omega_C = R_S \cdot \omega_S + R_P \cdot \omega_P \tag{3}$$

$$R_R \cdot \omega_R = R_C \cdot \omega_C + R_P \cdot \omega_P \tag{4}$$

$$R_C = R_S + R_P \tag{5}$$

$$R_R = R_C + R_P \tag{6}$$

The key effective kinematic constraint is given as:

$$(1+\xi_{RS}) \cdot \omega_C = \omega_S + \xi_{RS} \cdot \omega_R \tag{7}$$

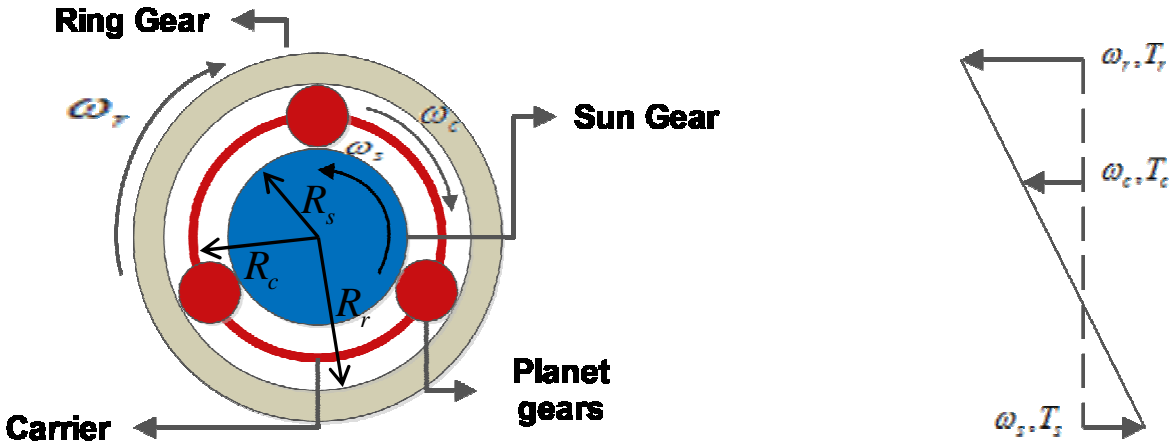

Fig. 5. Level diagram analogy of planetary gears.

The power split device is controlled by two actuators of brake band type. Each of them represents frictional brake with a flexible band that wraps around the periphery of a rotating drum to produce a braking action. A positive actuating force causes the band to tighten around the rotating drum and it places the friction surfaces in contact. The model employs a simple parameterization with readily accessible brake geometry and friction parameters according to the following relationship:

$$T_b = F_{in} \cdot \left(e^{\mu\varphi} - 1\right) \cdot \tanh\left(\frac{4\omega}{\omega_{th}}\right) \cdot r_d \tag{8}$$

The braking torque (T) is calculated according to required tension force (F_{in}) and is restricted by the contact friction coefficient (μ), wrap angle (φ) and the drum radius (r_d). (ω, ω_{th}) is the shaft angular and threshold speeds, respectively.

The control system monitors the throttle valve position signal and accordingly switches the motor/generator and outputs the brake band signals as given in Table

1. The brake bands are controlled via a slider gain that feed the input brake force to the model. The motor/generator switch either electrifies or ground the motor generator circuit. The model behaves instantaneously with parameters change, which enables the user to apply, and monitor changes in the model dynamics in real time. The controllers are joined together in a guide user interface (GUI) to provide a user friendly environment to control, monitor and judge the behavior of the system.

The vehicle body is assumed to be rigid with a lumped mass (m) which is concentrated at its center of gravity CG. The vehicle body has single degree of freedom which describes the vehicle longitudinal dynamics in x-direction. All forces affecting the vehicle body are shown in Figure 6-a, this includes gravity force (mg), front and rear tire forces (F_{xf}, F_{xr}), force due to road inclination (β) and aerodynamic drag (F_d). According to Newton's second law, the equation of motion in longitudinal direction is given as follows:

$$m \cdot \dot{V}_x = \left(F_{xf} + F_{xr}\right) - \frac{1}{2}\rho \cdot C_d \cdot A \cdot \left(V_x - V_D\right)^2 - m \cdot g \cdot \sin\beta \tag{9}$$

The generated tire forces are calculated according to Newton's second law as follows

$$I_w \cdot \dot{\Omega} = M_d - F_x \cdot r_d \tag{10}$$

The tire force (F_x) is calculated according to the following tire slip ratio, Figure 6-b

$$slip\ ratio = \frac{\Omega \cdot r_d - V_x}{\Omega \cdot r_d} \tag{11}$$

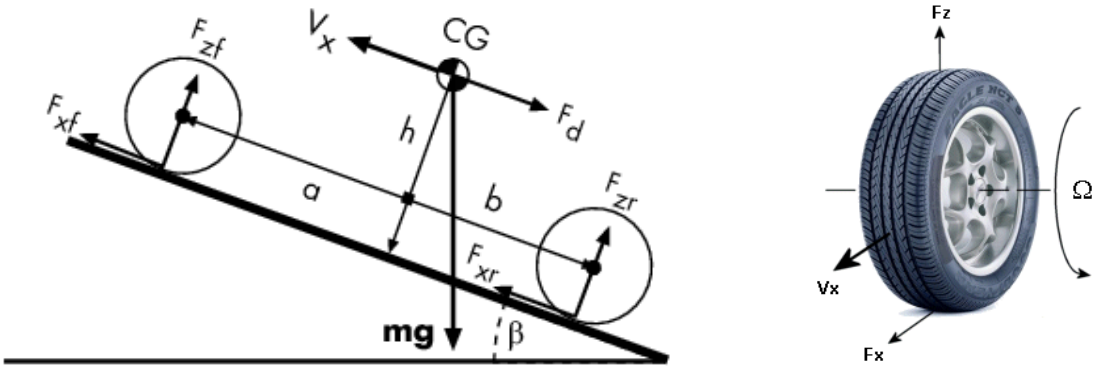

(a) Vehicle Body Forces (b) Tire Forces

Fig. 6. Vehicle Body Longitudinal Dynamics.

The presented model simulates the HEV operation during the acceleration and deceleration on straight and dry asphaltic flat road.

Table1: Modes of operation and control for the proposed model of HEV

Mode	Brake Band Sun	Brake Band Ring	Description
Charging	OFF	ON	Power is delivered from ICE to the carrier and then to the sun gear. The MG is driven to generate electric energy which is stored in the battery pack.
ICE only	ON	OFF	Power is delivered from ICE to the carrier and then to the ring gear. While the MG is off, ICE power drives the vehicle back axle.
Synergy	OFF	OFF	Power is delivered from ICE to the carrier and then to the ring gear. While the MG is on, power from both ICE and MG drive the vehicle back axle.

RESULTS AND ANALYSIS

Engine Drive Mode

In this state, the engine drives the vehicle without the aid of the MG output power. The MG switch is turned off and the brake band of the sun side BB2 is applied to prevent the engine power from leaking to the MG. the throttle is set to 30%. Figure 7 shows the engine speed accelerating from its idle speed at 800rpm to 1500rpm while the vehicle accelerating to its final speed.

MG Recharging Mode

The MG is driven by the engine in order to function as a generator. The vehicle is stopped and the whole engine output is used to drive the MG to charge the batteries. The brake band of the ring side BB1 is activated and that of the sun side BB2 is deactivated. The throttle valve is set to be 5% as expected in similar idle condition of the engine. Figure 8 shows the engine speed accelerating from its idle speed at 800rpm to 1100rpm which is the limit of the idle range, and the MG speed reaches 3850 rpm. The batteries initial state of charge are set to be 50%.

ICE-MG Synergy Mode

In this mode, both the ICE output and the MG output are used to empower the vehicle. Both brake bands of the sun and ring sides are deactivated so that they can deliver power to the vehicle at the same time. The throttle valve in this mode is set to 30% as in Engine Drive Mode, so the consumed power in both states can be compared. Figure 9 shows the engine accelerating to 1500rpm and the vehicle accelerating to 111.2m/s. A negative value of the MG rpm, which indicates its rotational direction to be opposite to those of ICE and Vehicle's propeller shaft.

A fairly comparison is carried out during the engine drive and synergy modes of operation. It is clear that, during the synergy mode, both fuel economy and driven mileage are improved as shown in Table 2.

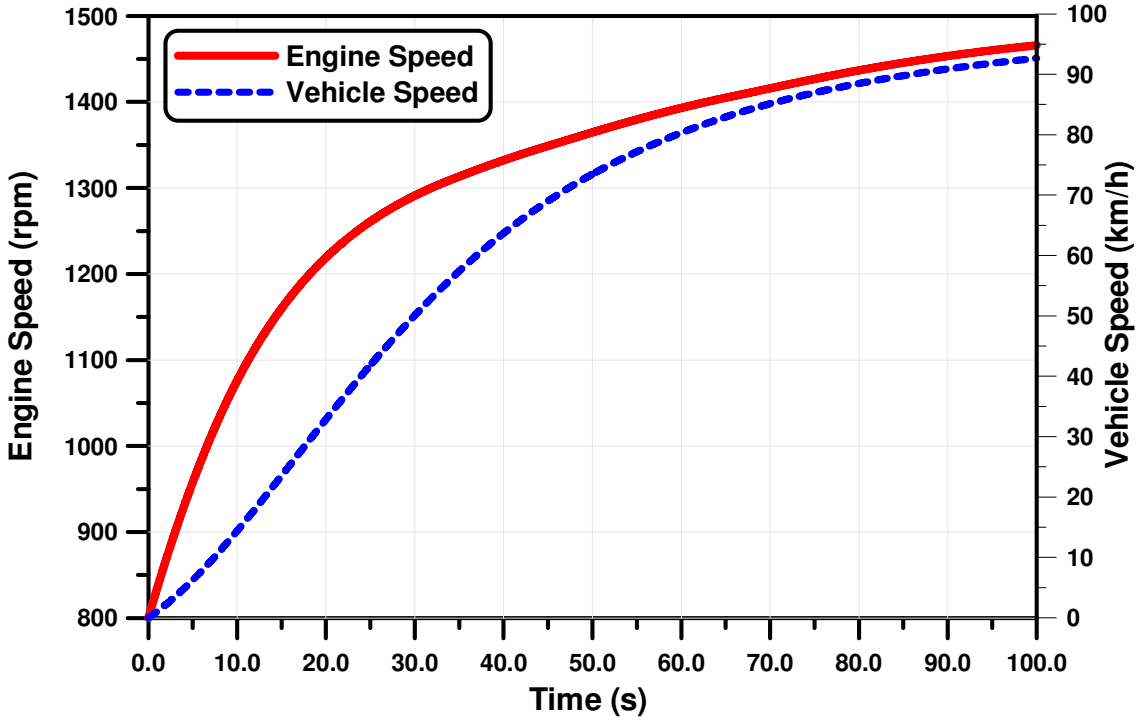

Fig. 7. Engine Drive Mode.

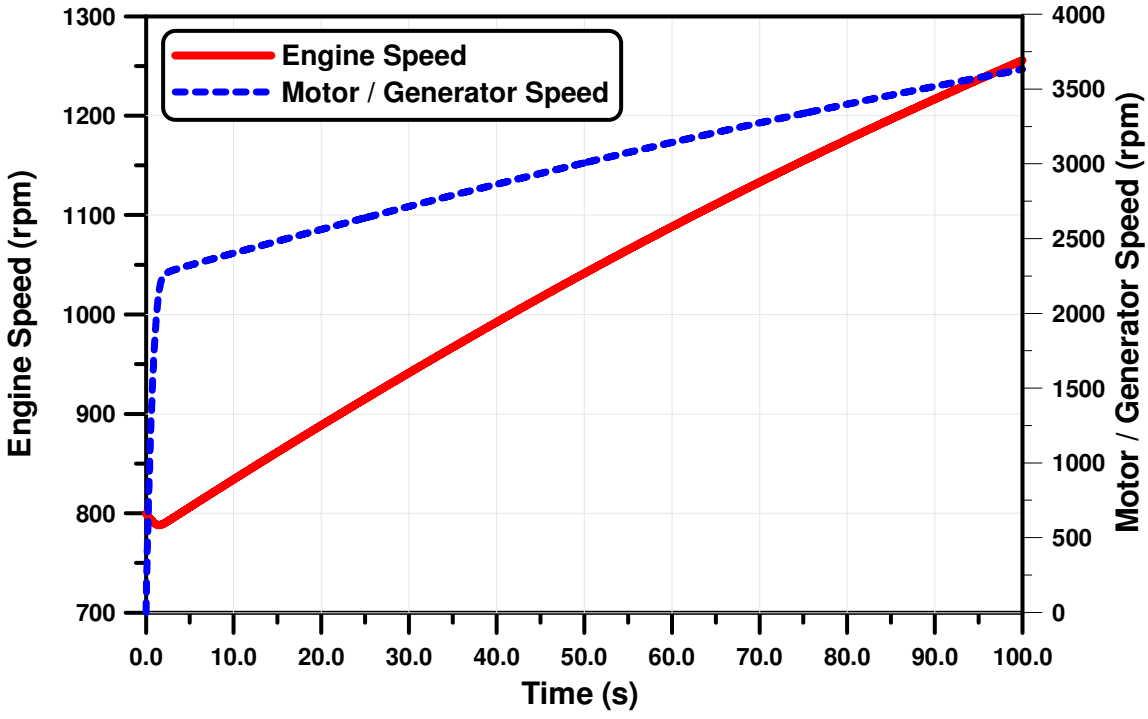

Fig. 8. Battery Recharging Mode.

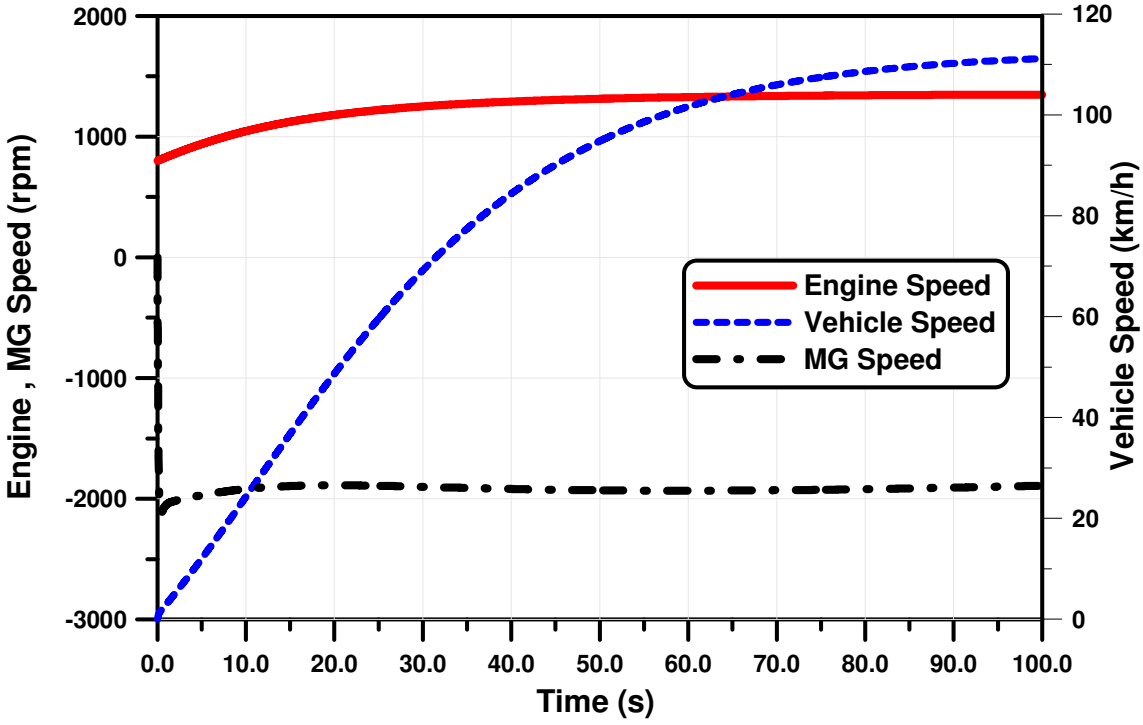

Fig. 9. Synergy Mode.

Table2: Fuel economy during the engine drive and synergy modes.

Mode	Engine drive mode	Synergy mode
Fuel Consumption (G/kW.Hr)	370.339	313.504
Mileage (Km/Liter)	11.676	16.653

CONCLUSIONS

Hybrid Electric Vehicles are one of the promising challenges in energy management applications. Exact simulation and control of the possible states of hybrid power train can achieve numerous virtues such as fuel consumption optimization and emissions reduction. The proposed model in this work shows some promising results for the different modes of operation matching the real case. As the model behaved in an accepted matter, many optimization and control methods can be applied on the model to experience their effect on the overall vehicle's efficiency.

REFERENCES

[1] The world Factbook, CIA, https://www.cia.gov/library/publications/the-world-factbook/, Last Updated: Apr 19, 2013

[2] U.S. Energy Information Administration, 'World liquid fuel supply and demand balance', Short-Term Energy Outlook, June– 2013,

[3] Jinming Liu and Huei Peng, 'Modelling and Control of a Power-Split Hybrid Vehicle, IEEE Transaction of Control Systems Technology, 2008, Vol.16, No.6

[4] Cristian Musardo, Giorgio Rizzoni, and Benedetto Staccia, 'A-ECMS: An Adaptive Algorithm for Hybrid Electric Vehicle Energy Management', 44th IEEE Conference on Decision and Control, and the European Control Conference, Barcelone, 2005, Spain.

[5] Manazir Ahmed Khan, 'Modelling and Simulation of Hybrid Electric Vehicles', International Journal of Mechanical and Production Engineering, 2013, Vol.1, Issue 3.

[6] Jinming Liu, Huei Peng and Zoran Filipi, 'Modeling and Analysis of the Toyota Hybrid System', International Conference on Advanced Intelligent Mechatronics, 2005, Monterey, California, USA.

[7] K. Muta, M. Yamazaki, and J. Tokieda, 'Development of new-generation hybrid system THS II—Drastic improvement of power performance and fuel economy', SAE, Warrendale, PA, Tech. Rep. 2004-01- 0064, 2004.

[8] T. Yaegashi, S. Abe, and D. Hermance, 'Future automotive powertrain—Does hybridization enable ICE vehicles to strive towards sustainable development', SAE, Warrendale, PA, Tech. Rep. 2004-21-0082, 2004.

[9] A. Kawahashi, 'A new-generation hybrid electric vehicle and its implication on power electronics', The Power Electron Seminar Ind. Rev. (CPES), Blacksburg, VA, Apr. 18–20, 2004.

[10] Paul Bowles, Huei Peng, Xianjie Zhang, 'Energy Management in a Parallel Hybrid Electric Vehicle With a Continuously Variable Transmission', American Control Conference, Chicago, Illinois, USA, 2000.

[11] Chan-Chiao Lin, Zoran Filipi, Yongsheng Wang, Loucas Louca, Huei Peng, Dennis Assanis and Jeffrey Stein, 'Integrated, Feed-Forward Hybrid Electric Vehicle Simulation in SIMULINK and its Use for Power Management Studies', SAE, 2001-01-1334, 2001.

[12] K.B. Wipke, M.R. Cuddy, and S.D. Burch, 'ADVISOR 2.1: A User-FriendlyAdvanced Powertrain Simulation Using a Combined Backward/Forward Approach, NREL/JA-540-26839, 1999.

[13] BMW 850i automatic (1991) full detailed specifications listing and photo gallery, http://www.automobile-catalog.com/auta_details1.php

[14] J. W. Wong, '*Theory of Ground Vehicle*', 2nd John Wiley, NY 1993.

[15] Tomas Gillespie, '*Fundamentals of Vehicle Dynamics*', SAE,1992

[16] Giancarlo Genta, '*Motor Vehicle Dynamics: Modelling and Simulation*', World Scientific Publishing Co. 1997. ISBN 98120229119

[17] S. Miller and J. Wendlandt. MATLAB News and Notes, 2010

[18] H. Benford and M. Leising, "The lever analogy: A new tool in transmission analysis," SAE, Warrendale, PA, Tech. Rep. 810102, 1981.

Appendix A: Vehicle and Simulation Parameters

The Vehicle		**The Engine**	
Vehicle gross mass (kg)	1200	Max. power (kw@rpm)	175@5000
No. of Driving Axles	2	Max. torque (N.m@rpm)	200@4000
Frontal Area (m^2)	3	Idle speed (rpm)	800
Wheel base (m)	3	Max. speed (rpm)	7000
Dynamic radius (m)	0.3		
Drag Coefficient	0.4		
Rolling res. coefficient	0.02		
Power Split Devise		**The Electric System**	
Type of planetary GB	Single row	Rated motor speed (rpm)	2000
Control Actuators	Brake bands	Rated motor power (kw)	25
Ring to sun ration	2	Rated DC voltage (v)	192
		Battery voltage (v)	192